



HAL
open science

Calculation of contraction coefficient under sluice gates and application to discharge measurement

Gilles Belaud, L. Cassan, Jean Pierre Baume

► **To cite this version:**

Gilles Belaud, L. Cassan, Jean Pierre Baume. Calculation of contraction coefficient under sluice gates and application to discharge measurement. *Journal of Hydraulic Engineering*, 2009, 135 (12), pp.1086-1091. 10.1061/(ASCE)HY.1943-7900.000012. hal-02596118

HAL Id: hal-02596118

<https://hal.inrae.fr/hal-02596118>

Submitted on 16 Nov 2023

HAL is a multi-disciplinary open access archive for the deposit and dissemination of scientific research documents, whether they are published or not. The documents may come from teaching and research institutions in France or abroad, or from public or private research centers.

L'archive ouverte pluridisciplinaire **HAL**, est destinée au dépôt et à la diffusion de documents scientifiques de niveau recherche, publiés ou non, émanant des établissements d'enseignement et de recherche français ou étrangers, des laboratoires publics ou privés.



OATAO is an open access repository that collects the work of Toulouse researchers and makes it freely available over the web where possible.

This is an author-deposited version published in : <http://oatao.univ-toulouse.fr/>
Eprints ID : 9010

To link to this article : DOI:10.1061/(ASCE)HY.1943-7900.0000122
URL : [http://dx.doi.org/10.1061/\(ASCE\)HY.1943-7900.0000122](http://dx.doi.org/10.1061/(ASCE)HY.1943-7900.0000122)
Open Archive TOULOUSE Archive Ouverte (OATAO)

<p>To cite this version : Belaud, Gilles and Cassan, Ludovic and Baume, Jean-Pierre <i>Calculation of Contraction Coefficient under Sluice Gates and Application to Discharge Measurement</i>. (2009) Journal of Hydraulic Engineering, vol. 135 (n° 12). pp. 1086-1091. ISSN 0733-9429</p>

Any correspondence concerning this service should be sent to the repository administrator: staff-oatao@listes.diff.inp-toulouse.fr

Calculation of Contraction Coefficient under Sluice Gates and Application to Discharge Measurement

Gilles Belaud¹; Ludovic Cassan²; and Jean-Pierre Baume³

Abstract: The contraction coefficient under sluice gates on flat beds is studied for both free flow and submerged conditions based on the principle of momentum conservation, relying on an analytical determination of the pressure force exerted on the upstream face of the gate together with the energy equation. The contraction coefficient varies with the relative gate opening and the relative submergence, especially at large gate openings. The contraction coefficient may be similar in submerged flow and free flow at small openings but not at large openings, as shown by some experimental results. An application to discharge measurement is also presented.

CE Database subject headings: Gates; Contraction; Coefficients; Hydraulic structures; Potential flow; Submerged flow; Free flow; Discharge measurement.

Introduction

Vertical sluice gates spanning the entire width, B , of a rectangular channel are among the most common structures in hydraulic engineering, and consequently have been much studied in the past (see Fig. 1 for a definition sketch). Attention has been mostly given to free flow conditions, and little theoretical work has been done for the submerged flow conditions that may frequently occur in open-channel networks. When gate openings are large, the head loss through the gate is small and the flow is largely submerged. Such conditions generally lead to large deviations between models and discharge measurements. One reason is, of course, the large uncertainty in the measurement of the difference between upstream and downstream water levels, but a variable contraction coefficient, C_c , may also play a role. Indeed, no contraction occurs when a submerged gate hardly penetrates the water stream. In this work, the variation of C_c under vertical sluice gates on horizontal beds is reexamined for free and submerged conditions.

Potential flow theory led to the analytic determination of C_c in free flow (von Mises 1917), based on conformal mapping between the physical plane and the complex potential plane (see review by Montes 1997). Using numerical methods, the effect of gate opening, W , on C_c was demonstrated (see e.g., Binnie 1952; Marchi 1953; Larock 1969; Fangmeier and Strelkoff 1968; among

others). More recently, Montes (1997) and Vanden-Broeck (1997) presented numerical solutions of this potential flow with an improved determination of the free surface, again in free flow.

Much less has been done for the submerged conditions. In fact, due to the lack of theoretical background, a common assumption is that C_c is the same in submerged flow as in free flow. Rajaratnam and Subramanya (1967) performed a detailed analysis of the flow structure under submerged sluice gates, up to $W=h_0/10$, where h_0 denotes the upstream depth. They pointed out the experimental difficulty of determining the contracted section in submerged flow but proposed a clear definition of the depth of the contracted stream based on the mass conservation. More recently and for radial gates, Tel (2000) noted that the vena contracta thickens at the beginning of submergence due to the pressure exerted on the jet. Using these observations and a review of existing works on submerged jets, Clemmens et al. (2003) introduced an energy correction to account for change in C_c at initial submergence.

A theoretical framework based on energy and momentum conservation, as well as on a recently developed description of pressure field on the upstream face of the gate, is proposed. The method leads to an analytic determination of C_c , both in free flows and submerged flows, and then to a discharge coefficient, C_d .

Energy and Momentum Balance

Energy Balance

Assuming no energy loss in the upstream pool, the water level on the upstream side of the gate H_0 is equal to the total head, E_0 , in section A (Fig. 1)

$$H_0 = E_0 = h_0 + Q^2/(2gB^2h_0^2) \quad (1)$$

in which Q =discharge; and g =acceleration due to gravity. Then, the energy conservation equation is written between section A and the contracted section (C). As done by Clemmens et al. (2003), a correction factor $k \geq 1$ may be introduced to account for kinetic energy correction and head loss

¹Assistant Professor, UMR G-EAU, SupAgro 1, place Pierre Viala, 34060 Montpellier Cedex 1, France (corresponding author). E-mail: gilles.belaud@supagro.inra.fr

²Researcher, UMR G-EAU, SupAgro 1, place Pierre Viala, 34060 Montpellier Cedex 1, France (corresponding author). E-mail: ludovic.cassan@supagro.inra.fr

³Research Engineer, UMR G-EAU, Cemagref, 361 rue Jean-François Breton, 34196 Montpellier Cedex 5, France. E-mail: jean-pierre.baume@cemagref.fr

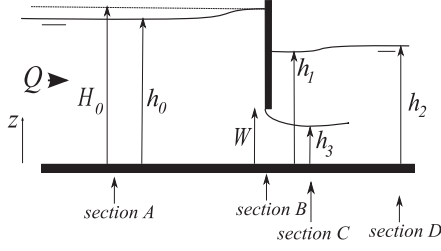


Fig. 1. Definition sketch for a submerged sluice gate

$$E_0 = h_1 + k \frac{Q^2}{2gB^2h_3^2} \quad (2)$$

where h_1 =depth at C and h_3 =thickness of the vena contracta. Clemmens et al. (2003) give experimental values of k with respect to the Reynolds number, and suggest values around 1.01–1.02 for field scale gates. Deviation from hydrostatic pressure in the vena contracta can also be considered. At section C, Rajaratnam and Subramanya (1967) showed that the pressure distribution deviates from hydrostatic pressure linearly with z

$$\Delta p \approx \lambda \left(1 - \frac{z}{h_3}\right) \rho \frac{Q^2}{2B^2h_3^2} \text{ for } 0 \leq z \leq h_3, \Delta p \approx 0 \text{ otherwise} \quad (3)$$

with $\lambda \approx 0.08$ (at a distance $x=1.25W$ from the gate in their runs), and ρ the mass density of water. Integrating with respect to z gives a correction factor of $1+\lambda/2$ on the kinetic energy. Hence, k may also account for pressure correction.

In dimensionless form, using $X=h_0/H_0$ (dimensionless upstream depth), $s=h_1/H_0$ (dimensionless downstream depth), $a=W/H_0$ (relative opening) and the upstream Froude number $F_0=Q/(B\sqrt{gh_0^3})$ leads to

$$F_0^2 = 2 \frac{a^2 C_c^2 (1-s)}{X^3 k} \quad (4)$$

$$X = 1 - \left(\frac{aC_c}{X}\right)^2 \frac{(1-s)}{k} \quad (5)$$

Momentum Balance

The momentum balance is applied in the x direction

$$\rho \frac{Q^2}{Bh_0} + \frac{1}{2} \rho g B h_0^2 + F_{gd} = \beta_u \rho \frac{Q^2}{Bh_3} + F_{pC} + F_{gu} \quad (6)$$

where F_{gd} , F_{gu} , and F_{pC} =pressure forces on the downstream face of the gate, on its upstream face, and at section C, respectively; and β_u =momentum correction factor.

On the downstream face of the gate, above the jet, the velocity magnitude is small, and therefore the pressure can be assumed hydrostatic (Rajaratnam and Subramanya 1967)

$$F_{gd} = \frac{1}{2} \rho g B (h_1 - W)^2 \quad (7)$$

with $\epsilon=1$ if $h_1 > W$, $\epsilon=0$ if $h_1 \leq W$.

The pressure force at the contracted section is written taking account of pressure correction

$$F_{pC} = \frac{1}{2} \rho g B h_1^2 + \frac{1}{2} \lambda \rho \frac{Q^2}{2Bh_3} \quad (8)$$

The pressure force on the upstream face, F_{gu} , is obtained from a closed-form expression for the potential velocity upstream of a rectangular contraction (Belaud and Litrico 2008). The method assumes that the horizontal velocity is uniform under the gate, which is verified whether in free flow or in submerged flow (Rajaratnam and Subramanya 1967). In the case of a gate on a horizontal bed, the vertical component of the velocity on the upstream face of the gate, $v(z)$, is given by

$$v(z) = -\frac{Q}{\pi W B} \log \left(\frac{\sin \frac{\pi(z+W)}{2H_0}}{\sin \frac{\pi(z-W)}{2H_0}} \right) \quad (9)$$

Applying the Bernoulli theorem yields the dimensionless pressure, $\tilde{p} = p/\rho g H_0$

$$\tilde{p}(\tilde{z}) = 1 - \tilde{z} - \frac{1}{2\pi^2} \frac{F_0^2 X^3}{a^2} \left[\log \left(\frac{\sin(\pi(\tilde{z}+a)/2)}{\sin(\pi(\tilde{z}-a)/2)} \right) \right]^2 \quad (10)$$

where $\tilde{z}=z/H_0$. Eq. (10) yields $\tilde{p} \rightarrow -\infty$ when $\tilde{z} \rightarrow a$. The physical limit of validity is given by $\tilde{p} = \tilde{p}_0$, where \tilde{p}_0 =dimensionless gauge pressure exerted on the jet when it separates from the gate. This pressure is given by continuity of the pressure exerted downstream from the gate. As long as $h_1 < W$, such as in free flow, $\tilde{p}_0=0$, otherwise the hydrostatic assumption on the downstream face leads to $\tilde{p}_0=s-a$. Belaud and Litrico (2008) showed that the value z_l for which $p(z_l)=0$ (in free flow) is very close to W . This approximation is easily extended to submerged conditions

$$\tilde{z}_l \approx a + \frac{2 \sin(\pi a)/\pi}{\exp\left[\frac{\pi \tilde{d}}{C_c \sqrt{1-s}}\right] - \cos(\pi a) - \frac{\sin(\pi a)}{C_c \sqrt{1-s \tilde{d}}}} \quad (11)$$

where $d=1-a-\tilde{p}_0$. When $h_1 > W$, $d=1-s$, otherwise $d=1-a$. Note that \tilde{z}_l is a function of C_c , a , and s . By making use of trigonometric identities and the change of variables $t = \tan(\pi z/2H_0)/\tan(a\pi/2)$ and $t_l = \tan(\pi z_l/2H_0)/\tan(a\pi/2)$, integration of Eq. (10) is expressed in dimensionless form as

$$\tilde{F}_{gu} = (1-a)^2 - 2F_0^2 X^3 \phi(a, t_l) \quad (12)$$

where

$$\phi(a, t_l) = \frac{\tan(a\pi/2)}{\pi^3 a} \int_{t_l}^{\infty} \frac{1}{1 + \tan^2(a\pi/2)t^2} \log^2 \left(\frac{t+1}{t-1} \right) dt \quad (13)$$

The dimensionless momentum equation is obtained from Eq. (6) as

$$2F_0^2 X^2 + X^2 + \epsilon(s-a)^2 = 2 \frac{F_0^2 X^3}{a C_c} + s^2 + \frac{\lambda F_0^2 X^3}{2 a C_c} + (1-a)^2 - 2 \frac{F_0^2 X^3}{a} \phi(a, t_l) \quad (14)$$

Combining Eqs. (4), (5), and (14) leads to

$$4X - 3X^2 + \epsilon(s-a)^2 = (4+\lambda) \frac{\beta_u}{k} a C_c (1-s) + s^2 + (1-a)^2 - \frac{4}{k} a C_c^2 (1-s) \phi(a, t_l) \quad (15)$$

Solving the system of Eqs. (5)–(15) leads to the values of C_c and X as functions of a and s . The effect of λ on momentum is, to some extent, counterbalanced by its effect on energy, and the

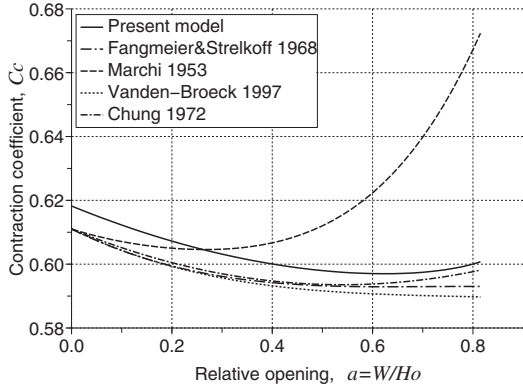


Fig. 2. Contraction coefficient as a function of relative opening a in free flow

same for velocity distribution at section C. Therefore, most corrections can be considered through coefficient k , setting $\lambda=0$ and $\beta_u=1$. We now distinguish the free flow conditions ($s=a$) and two regimes in submerged flow, according to the value of ϵ .

Contraction Coefficient in Free Flow

In this case the water level h_1 is equal to $h_3=C_c W$ and $F_{gd}=0$. Therefore, we have $\epsilon=0$ and $s=h_1/H_0=aC_c$. In the limiting case, $a \rightarrow 0$, the solution of Eqs. (15) and (5) is found as $C_c=C_{c0}=0.6182$ which is close to that obtained by the conformal mapping method ($\pi/(\pi+2) \approx 0.611$), the slight difference being explained by the different assumptions made for the potential solution. For finite a , Eqs. (15) and (5) are valid until $h_0 > W$ ($X > a$), which corresponds to a mathematical limit of $a \approx 0.815$, $F_1=1.44$, and $F_0 \approx 0.7$. This is higher than the physical limit identified by Montes (1997) who reports free surface instabilities for $a > 0.5$ and a physical limit of $a \approx 0.6$ ($F_1 \approx 1.9$).

The variation of C_c with a are compared in Fig. 2 with the numerical results of Fangmeier and Strelkoff (1968), Vanden-Broeck (1997), Marchi (1953), and Chung (1972). C_c decreases when a increases from 0–0.5, then slightly increases for larger values of a . The minimum value of C_c is slightly below 0.6. The results presented here are also very close to those presented by Montes (1997).

Experimental values of C_c are generally higher than the theoretical predictions, as illustrated on Fig. 3 with the data provided by Fawer (1937), Rajaratnam (1977), and Defina and Susin (2003). This is particularly true at smaller laboratory scales where fluid viscosity, surface tension, relative boundary roughness, and exact geometry may be of importance (Speerli and Hager 1999). The main energy loss is due to friction in the boundary layers, especially in the vena contracta and near the separation point. These effects are all the higher when the gate Reynolds number is low (Roth and Hager 1999; Clemmens et al. 2003), which leads to scale effects between laboratory data and field data. Also, the relative importance of the boundary layer in the vena contracta affects the velocity distribution, and therefore the downstream kinetic energy (Ohtsu and Yasuda 1994). The influence of the corner vortices and eddies in the upstream recirculation zone should be considered too. The energy transferred to turbulence by these large scale structures are not necessarily dissipated before the contracted section. However, the velocity distribution can be affected even if the total energy (mean kinetic plus turbulent ki-

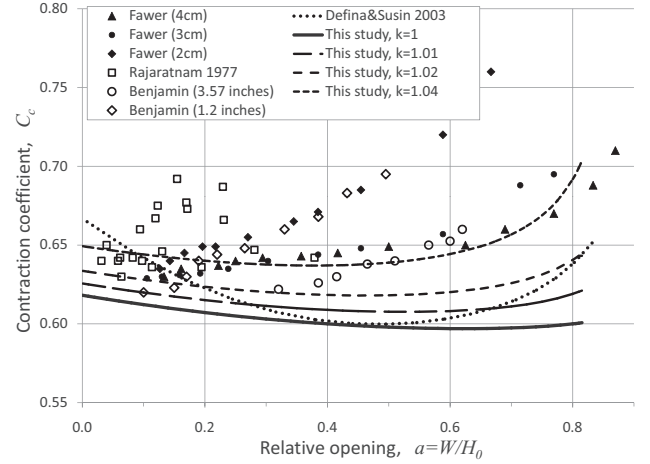


Fig. 3. Contraction coefficient in free flow: Experimental data by Defina and Susin (2003); Fawer (1937); Benjamin (1956); Rajaratnam (1977) (dots) and present model with different values of correction factor k on the downstream kinetic energy. The dotted line is the best fitting proposed by Defina and Susin (2003).

netic energy) is roughly constant. These effects may be considered in the correction factors. Fig. 3 illustrates the effect of k for values up to 1.04 (which corresponds to a kinetic energy correction of 4%), showing that consistent and plausible values of k can be fitted to experimental data. Experimental observations and numerical simulations (Kim 2007) also suggest to consider a head loss in the conversion of kinetic energy in the upstream pool. In simulations for free flow of Kim (2007), the conversion is correct up to $a \approx 0.4$ but head loss appears above this value. He obtained contraction coefficients between 0.618 and 0.630.

Contraction Coefficient in Submerged Flow

Analytical Formulation

From Eq. (14), C_c should be modified compared to free flow. Two different regimes must be distinguished according to the value of ϵ . We define the partially submerged flow as the regime where the vena contracta is drowned ($h_1 > C_c W$) but the downstream water level does not reach the gate ($h_1 < W$). In this case, $F_{gd}=0$ and $\epsilon=0$. This regime occurs when the downstream water level (far from the gate) is increased progressively from the free flow regime.

A fully submerged flow occurs when h_1 reaches the downstream side of the gate. In this case, $h_1 > W$ ($s > a$) and $\epsilon=1$, and Eq. (15) reduces to

$$a(3X-1) \frac{C_c^2}{2X^2} = 2C_c - 1 - 2C_c^2 \phi(a, t) \quad (16)$$

Fig. 4 gives the values of C_c in the plane (a, s) for all regimes. The line $s=a$. C_c gives the limit between free flow and submerged flow, while $s=a$ is the limit between partially and fully submerged flow. For small a , $C_c \approx C_{c0}$ even for high s . Indeed, setting $a=0$ in Eq. (16) leads to the same equation as in free flow. When $a=0.5$, C_c is much more sensitive to s , and its value remains above 0.65 when $s > 0.5$. In this case, C_c is about 10% higher than in free flow at the same opening. At a much larger opening

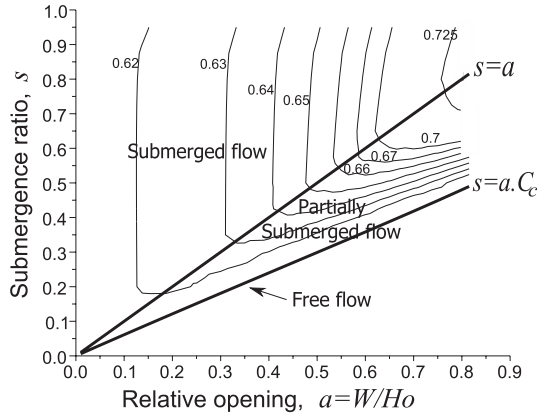


Fig. 4. Flow regime and C_c in plane (a, s)

($a=0.8$), this deviation from the free flow reaches a maximum of 25%.

Effect of Gate Opening on C_c

For different fixed values of $s=h_1/H_0$, C_c is plotted as a function of the relative opening a (Fig. 5). Unlike in free flow, C_c tends to increase when a increases. Then, when the flow becomes partially submerged, C_c slightly decreases to reach the free flow value when $a=s/C_c \approx 1.67 s$. In fully submerged flow ($s > a$), s has little influence on C_c . The influence is due to the function $\phi(a, t_1)$ in which t_1 depends on s , but the variation of ϕ with s is small compared to its variation with a . A good approximation of ϕ , calculated numerically with $C_c=C_{c0}$, $s=0.95$ is given by

$$\phi(a, t_1) \approx \Phi(a) = 0.194a^2 - 0.499a + 0.308 \quad (17)$$

Setting $X=1$ in Eq. (16) and $\phi(a, t_1) \approx \Phi(a)$ gives the following approximation:

$$C_c \approx \frac{1 - \sqrt{1 - (2\Phi(a) + a)}}{2\Phi(a) + a} \quad (18)$$

Some experimental results confirm the increase of C_c with a for submerged flow, such as Woycicki (1935) who proposed the following relation:

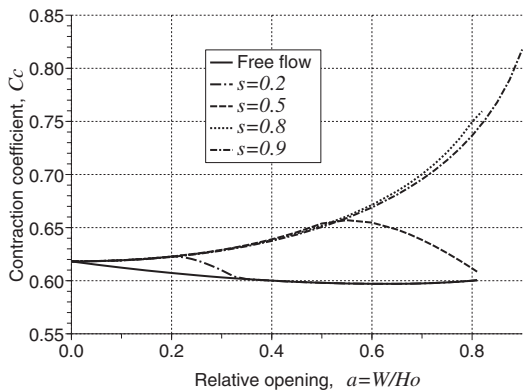


Fig. 5. Variation of C_c as a function of relative gate opening $a=W/H_0$. Different downstream conditions are applied: free flow, $s=0.2$, $s=0.5$, $s=0.8$, and $s=0.9$.

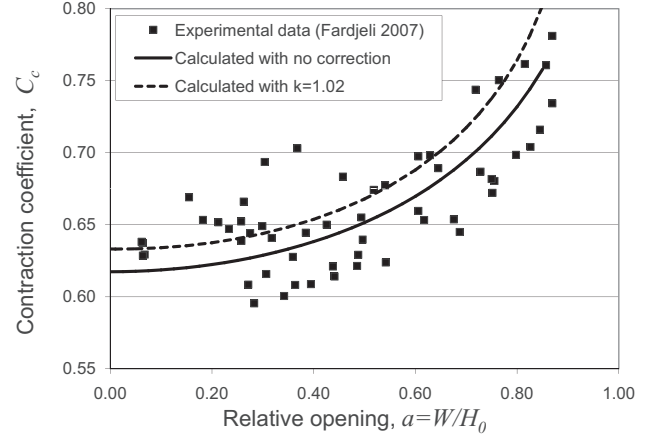


Fig. 6. Experimental results for C_c in submerged flow (dots), predicted C_c without correction (plain line) and with $k=1.02$ (dashed line), and the data set of Fardjeli (2007)

$$C_c = 0.617 + 0.04a \quad (19)$$

For large opening and large submergence, higher values of C_c are expected. This domain was explored experimentally by Fardjeli (2007). The canal is 30-cm-wide with a maximal depth of 45 cm. Discharge was measured using a calibrated V-notch weir and water levels were measured using point gauges. The discharge was set at two different values, 16 and 30 l/s. For each discharge, five gate openings were used (3, 6, 12, 20, and 30 cm). Different water levels were controlled by a downstream sluice gate. The experimental C_c was estimated indirectly from Eq. (2), and is plotted with respect to a on Fig. 6. Although some discrepancy appears in the relation, the trend is well reproduced by Eq. (18). As for free flow, correction factors may be used to account for simplifications, such as no energy loss, hydrostatic pressure and nonuniform velocity in contracted section. Although these assumptions are justified by a few experimental results of Rajaratnam and Subramanya (1967), more investigation is needed to quantify them and modify the corresponding forces and momentum accordingly. As for free flow, increasing k tends to increase C_c , as shown in Fig. 6 with $k=1.02$.

Effect of Downstream Level h_2

The previous calculations used h_1 rather than h_2 . This is physically justified since h_1 is more representative of the flow conditions that prevail in the vicinity of the vena contracta. The use of h_2 is often preferred since it is less variable, whereas h_1 should be filtered. While both quantities are almost equal at large submergence, they largely deviate as s becomes small. The link between h_1 and h_2 depends on the downstream pool characteristics. In particular, if several gates flow in parallel, they should have the same h_2 but may be not the same h_1 .

To illustrate the effect of h_2 , a rectangular downstream channel is considered. The momentum principle leads to

$$s = \sqrt{s'^2 + 4a^2 C_c^2 (1-s)} \left(\frac{1}{s'} - \frac{1}{a C_c} \right) \quad (20)$$

where $s'=h_2/H_0$. Fig. 7 shows the variations of s and C_c with s' for $a=0.2$, $a=0.4$, and $a=0.6$. The appearance of partially submerged flow, as h_2 increases, is clearly visible. For a fully submerged flow, C_c is almost constant. Considering three gates in

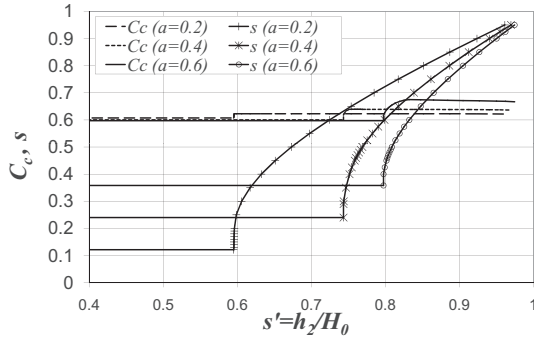


Fig. 7. Variation of C_c and s with $s' = h_2/H_0$, $a = 0.2$, $a = 0.4$, and $a = 0.6$

parallel with different gate openings, such as on Fig. 7, h_2 (and s') can be the same, but the contraction coefficient can be significantly different. Taking $s' = 0.85$ gives variations of 10% on C_c between $a = 0.2$ and $a = 0.6$, and s values of 0.66 and 0.80, respectively, both effects leading to discharge four times larger for $a = 0.6$ than for $a = 0.2$.

Application to Discharge Measurement

Assuming that W and H_0 are measured, as well as h_1 in submerged flow, a and s are calculated. The flow regime is determined, and then C_c using Eqs. (5) and (15). Alternatively, C_c can be determined from Fig. 4. The discharge is calculated from the energy equation

$$Q = \frac{C_c}{\sqrt{k}} WB \sqrt{2g(H_0 - h_1)} \quad (21)$$

with $h_1 = C_c W$ in free flow. The coefficient k can be considered as a calibration coefficient. However, $k > 1$ increases C_c to some extent, and therefore its sensitivity is rather limited.

The approach is applied to well known experimental results of Henry (1950) (see Fig. 8). Since h_2 is used rather than h_1 , Eq. (20) is used. The present method slightly overpredicts the discharge coefficient. A k factor of 1.05 in Eq. (21) gives an excellent superposition with Henry's curves, which means that the present

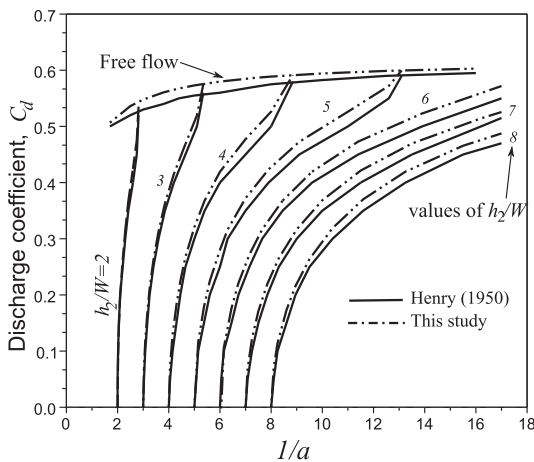


Fig. 8. Application of present method to experimental results of Henry (1950)

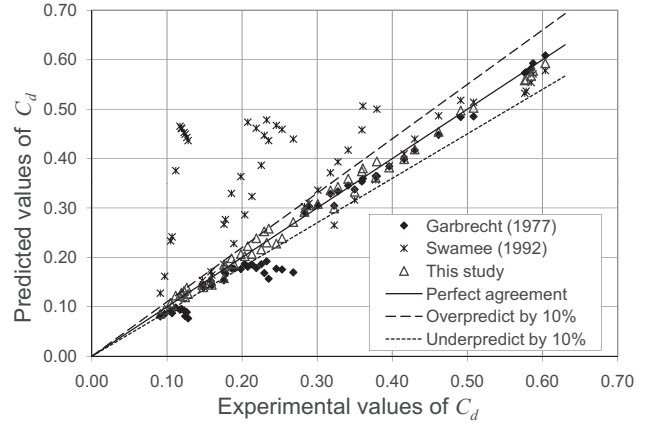


Fig. 9. Predicted values of discharge coefficient C_d with the model of (diamonds) Garbrecht (1977), formula (crosses) of Swamee (1992), and present model (triangles), versus experimental values using the data set of Fardjeli (2007)

method overpredicts the discharge coefficient by about 2.5%. In these curves, however, large openings ($a \geq 0.5$) were little explored. The performance of the method is also evaluated on the data set of Fardjeli (2007). The formulas of Garbrecht (1977) and Swamee (1992) were applied too. Swamee's formula performs poorly in the studied domain (Fig. 9) as can be expected from its mathematical formulation, obtained by fitting on Henry's curves where $a \leq 0.5$. In particular, Swamee's formula gives no solution for $a \geq 0.81^{1/0.72} \approx 0.746$. The formulation proposed by Garbrecht (1977) performs better, except for lower values of C_d , corresponding to large submergence. Using the present method gives the best results, all prediction errors being lower than 10%.

Conclusion

We proposed a new theoretical framework for the calculation of contraction coefficients under sluice gates on flat bed. The approach, based on momentum and energy conservation between the upstream pool and the contracted section, relies on an analytical calculation of the pressure field upstream of the sluice gate.

In free flow, results are consistent with published results. The study was extended to submerged conditions, for which few theoretical results are available. A partially submerged regime was defined to occur when the vena contracta is drowned but the downstream water body does not touch the downstream side of the gate. In submerged flow, C_c remains close to its free flow value when the relative gate opening is small whatever the submergence, which confirms experimental results and a generally admitted assumption. This is no longer valid at large opening, where C_c can be much higher than 0.6, provided the flow is sufficiently submerged. In this case, the value of C_c depends little on the submergence. Such a variation of C_c should be taken into account when calculating the flow through a largely open and largely submerged gate, for modeling or measuring purpose for instance. Experimental results confirm such variation with gate opening. The method is then applied to discharge calculation with good results, especially at large opening and large submergence.

The approach can be directly used to gates with a sill, possibly with a different height in the upstream and downstream pools. For that, additional pressure forces need to be included in the momen-

tum balance. Also, real fluid effects may be of importance in some regimes. Such effects can be introduced using correction coefficients in energy and momentum equations.

Notation

The following symbols are used in this technical note:

- a = relative gate opening= W/H_0 ;
- B = gate or channel width;
- C_c = contraction coefficient= h_3/H_0 ;
- C_{c_0} = contraction coefficient for $a=0$;
- E_0 = upstream energy;
- F_p = pressure force;
- F_0 = Froude number at the upstream section
= $Q/(B\sqrt{gh_0^3})$;
- g = gravity constant= 9.81 m/s^2 ;
- H_0 = depth (also head) on the upstream face on the gate;
- h_0 = upstream depth or level;
- h_1 = downstream depth or level (immediately downstream of the gate);
- h_2 = downstream depth or level (far from the gate);
- h_3 = thickness of the vena contracta;
- k = coefficient for energy correction;
- p = pressure;
- \bar{p} = dimensionless pressure= $p/(\rho g H_0)$;
- Q = discharge through the gate;
- s = submergence ratio= h_1/H_0 ;
- t_1 = relative limit for pressure integration;
- v = vertical velocity component;
- W = gate opening;
- X = dimensionless upstream depth= h_0/H_0 ;
- z = elevation;
- \tilde{z} = dimensionless elevation= z/H_0 ;
- z_l = lower limit of z for pressure integration;
- α = correction coefficient on energy;
- β_u = correction coefficient on momentum;
- ϵ = 1 if $h_1 > W$, $\epsilon=0$ if $h_1 \leq W$;
- λ = correction coefficient on pressure distribution; and
- ρ = mass density.

References

Belaud, G., and Litrico, X. (2008). "Closed-form solution of the potential flow in a contracted flume." *J. Fluid Mech.*, 599, 299–307.

- Benjamin, T. B. (1956). "On the flow in channels when rigid obstacles are placed in the stream." *J. Fluid Mech.*, 1, 227–248.
- Binnie, A. (1952). "The flow of water under a sluice gate." *Q. J. Mech. Appl. Math.*, 5, 395–407.
- Chung, Y. (1972). "Solution of flow under sluice gates." *J. Engrg. Mech. Div.*, 98(1), 121–140.
- Clemmens, A., Strelkoff, T., and Replogle, J. (2003). "Calibration of submerged radial gates." *J. Hydraul. Eng.*, 129(9), 680–687.
- Defina, A., and Susin, F. (2003). "Hysteretic behavior of the flow under a vertical sluice gate." *Phys. Fluids*, 15, 2541–2548.
- Fangmeier, D., and Strelkoff, T. (1968). "Solution for gravity flow under a sluice gate." *J. Engrg. Mech. Div.*, 94(EM1), 153–176.
- Fardjeli, N. (2007). "Modélisation d'ouvrages de régulation pour l'aide à la gestion des canaux." MS thesis, Montpellier Supagro, France, 57 (in French).
- Fawer, C. (1937). "Etude de quelques écoulements permanents à filets courbes." Ph.D. thesis, EPF Lausanne, Switzerland (in French).
- Garbrecht, G. (1977). "Discussion of 'Discharge computations at river control structures' by L. Dannie." *J. Hydr. Div.*, 103(2), 1481–1484.
- Henry, R. (1950). "Discussion to 'On submerged jets.'" *Trans. ASCE*, 115, 687–694.
- Kim, D. (2007). "Numerical analysis of free flow past a sluice gate." *KSCE J. Civil Engineering*, 11(2), 127–132.
- Larock, B. (1969). "Gravity-affected flow sluice gate." *J. Hydr. Div.*, 95(HY4), 153–176.
- Marchi, E. (1953). "Sui fenomeni di efflusso piano da luci a battente." *Ann. Mat. Pura Appl.*, 35(1), 327–341 (in Italian).
- Montes, J. S. (1997). "Irrotational flow and real fluid effects under planar sluice gates." *J. Hydraul. Eng.*, 123(3), 219–232.
- Ohtsu, I., and Yasuda, Y. (1994). "Characteristics of supercritical-flow below sluice gate." *J. Hydraul. Eng.*, 120(3), 332–346.
- Rajaratnam, N. (1977). "Free flow immediately below sluice gates." *J. Hydr. Div.*, 103(4), 345–351.
- Rajaratnam, N., and Subramanya, K. (1967). "Flow immediately below submerged sluice gate." *J. Hydr. Div.*, 93(4), 57–77.
- Roth, A., and Hager, W. (1999). "Underflow of standard sluice gate." *Exp. Fluids*, 27, 339–350.
- Speerli, J., and Hager, W. (1999). "Discussion to 'Irrotational flow and real fluid effects under planar sluice gates' by J.S. Montes." *J. Hydraul. Eng.*, 125(2), 208–210.
- Swamee, P. (1992). "Sluice gate discharge equations." *J. Irrig. Drain. Eng.*, 118(1), 56–60.
- Tel, J. (2000). "Discharge relations for radial gates." MS thesis, Delft Technical Univ., The Netherlands.
- Vanden-Broeck, J. (1997). "Numerical calculations of the free-surface flow under a sluice gate." *J. Fluid Mech.*, 330, 339–347.
- von Mises, R. (1917). *Berechnung von ausfluß und ueberfallzahlen*, Zeitschrift des Vereines Deutscher Ingenieure, Berlin (in German).
- Woycicki, K. (1935). "The hydraulic jump on its role on discharge of sluice gates." *Technical Rep. No. 3-2*, U.S. Bureau of Reclamation, Denver, 65.